Alternate Multihop Routing in Limited Reconfigurable Optical Networks

Onur Turkcu and Suresh Subramaniam
Department of Electrical and Computer Engineering
The George Washington University
Washington, DC 20052
Email: {onurturk, suresh}@gwu.edu

***Abstract*—In this paper, we investigate the performance of limited reconfigurable optical networks when multihopping is used. Multihopping is achieved by dropping a wavelength at an intermediate node and transmitting on another wavelength at that node (O-E-O). A route can consist of several such hops each obeying the *wavelength continuity constraint* individually. Considering that a receiver and a transmitter are used for add/drop at a node, multihopping is restricted by the number of transponders and their tunabilities. We develop a dynamic routing strategy based on the availability and tunability of transponders as well as the wavelength availability. We adopt a Share-Per-Link model for the usage of transponders within a reconfigurable node, and each node is assumed to be equipped with a ROADM which can add/drop any wavelength to any of the ports. We show that the proposed routing strategy improves the blocking performance significantly compared to fixed routing with or without multihopping or alternate routing methods without multihopping.**

I. Introduction

Reconfigurable optical networks allow dynamic adjustment of the lightpaths established in the network. Reconfigurability requires Reconfigurable Optical Add/Drop Multiplexers (ROADMs) and tunable transponders. On the arrival of a lightpath request, the network tries to establish the lightpath by reconfiguring ROADMs to add/drop different wavelengths and tuning the transponders to required wavelengths at the terminal nodes. Such a call establishment generally requires an end-to-end available wavelength (*wavelength continuity constraint*) when there is no wavelength conversion. A new constraint called *wavelength termination constraint* was introduced in [1] which additionally requires available transponders on both source and destination nodes that can tune to the end-to-end available wavelength. We consider limited tunable transponders (LTTs) which can tune to a certain wavelength range in the entire spectrum and that each LTT is assigned a waveband (the entire spectrum is assumed to be partitioned into non-overlapping wavebands). LTTs are currently available in the market by several equipment providers. For example, Finisar have tranceievers using chirp-managed laser technology called CML tranceivers (model no. DM80-01-3/4, DM200-01-3/4) which can tune to 2, 4 or 8 wavelengths within the C-band or the L-band [2]. Customers can order such tranceivers that are tunable to their wanted wavebands. It is shown in [1], [3] that LTTs are sufficient to give the same blocking performance as widely tunable transponders (WTTs). Moreover, in [4] it is shown that LTTs result in more inventory savings than WTTs. However, in the case of LTTs if the terminal nodes of a lightpath request do not have transponders that can tune to the same waveband, then that lightpath cannot be established. In [5], we proposed algorithms for assigning wavebands to transponders so that they share more common wavebands and these methods were shown to reduce the blocking.

In this paper, we consider wavelength conversions occurring at intermediate nodes by O-E-O. An intermediate node can drop a certain wavelength, and transmit on another wavelength. It does this by electronically connecting the drop port to the add port. We call this scheme *multihopping*. We note that at each intermediate node two transponders are required: one for drop and one for add. With wavelength conversions, the entire path does not have to be wavelength-continuous but instead each hop is wavelength-continuous individually. All-optical wavelength conversion is studied in [6] which proposes having wavelength conversion only in a subset of the nodes in the network. In [7], the authors consider wavelength conversion within a multi-granular optical crossconnect (MG-OXC) and a heuristic is proposed for dynamic traffic to reduce the blocking probability by efficiently routing and assigning wavelengths to new lightpath requests and grouping them into bands such that the number of used wavelength converters is reduced. Routing and wavelength assignment algorithms are proposed in [8] for the MG-OXC architecture with an objective of minimizing the number of ports needed by the MG-OXCs. In [9], the hybrid hierarchical switch consisting of an optical crossconnect for waveband routing and an O-E-O switch is introduced. O-E-O switch is used for wavelength routing and, similar to our case, for wavelength conversion. The authors evaluate the throughput performance and the cost depending on the size of the switch which takes into account the number of transponders in the O-E-O switch. An RWA algorithm is introduced in [10] to be used in the presence of sparse or/and full wavelength conversion that reduces the blocking compared to other RWA algorithms.

The effect of multihopping has not been investigated when LTTs are employed in the network. The number of transponders is one constraint on multihopping since allowing too many hops will exhaust available transponders. On the other hand, with LTTs not every conversion from a wavelength to another is possible (there should be a LTT tunable to the

dropped wavelength and also another LTT tunable to the added wavelength). Our goal is to find out how advantageous it is to use multihopping with LTTs. In this paper, we develop a graph model based on the constraints of LTTs to calculate a route for a lightpath request. Our model not only finds a possible route with our without multihopping, but also chooses the best multihop route on which transponder resources are the least exhausted. We also note that the poor blocking performance due to the mismatch of wavebands of the transponders at different nodes can be eliminated by the use of multihopping. We illustrate this case with an example in Fig.1. We show by small rectangles the available transponders in the node and the numbers denote the wavelengths that they can receive/transmit. (The sizes of the wavebands of LTTs are 1 in this example, i.e., these are fixed transponders). Here, all 4 wavelengths are available along a two-hop route. However, the source node can only transmit on the wavelengths 1 and 2 whereas the destination node can only receive at wavelengths 3 and 4. Even though there is an end-to-end wavelength-continuous path in this case, a lightpath cannot be established due to the wavelength termination constraint. If we allow multihopping, the intermediate node can drop the first wavelength and then add the fourth wavelength using all of its available transponders. Hence, a multihopped lightpath can be established by using wavelength 1 and 4 in the first and second links, respectively.

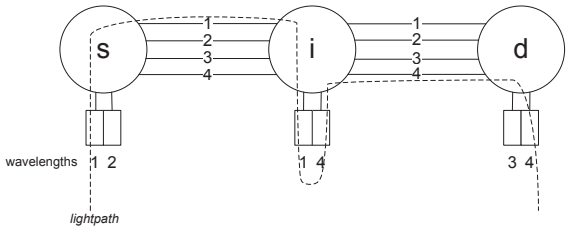

Fig. 1. Example of multihopping.

The rest of the paper is organized as follows. In Section II, we describe the network model. In Section III, the graph model for alternate multihop routing is explained in detail. We provide simulation results to evaluate the performance of the new routing algorithm in Section IV, and we conclude the paper in Section V.

II. Network Model

There are N nodes in the network numbered as $1, \ldots, N$, and L bidirectional links interconnecting them (i.e., each link has two fibers in opposite directions) numbered as $1, \ldots, L$. Each fiber carries W wavelengths numbered as $1, \ldots, W$. Each node is equipped with a fully reconfigurable multidegree ROADM with colorless ports. We adopt a Share-Per-Link model for the usage of transponders within a node. In this model, each link has its own dedicated transponders. The number of transponders that a node has is T per link. Each LTT is assigned to a waveband of size Θ. There are B non-overlapping wavebands where $B = W/\Theta$. We assume B to be an integer. D_n denotes the number of links that a node n is connected to, or the degree of node n. We denote the set of transponders for a degree t of a node n by T_n^t where $t = 1, \ldots, D_n$. All lightpath requests are bidirectional and established on the same wavelength in both directions. Lightpath requests arrive in a Poisson fashion and they have exponential holding times. We show a 2-degree ROADM in Fig. 2 as an example. A lightpath can be dropped using the receiver of link 1 (T_n^1) and added using transmitter of the link 2 (T_n^2) for lightpath 1; or it can be added/dropped by the transmitter/receiver of the link 1 (T_n^1), hence routed back on the same link as lightpath 2. We note that this requires the use of an O-E-O switch (not shown in the figure) that allows any receiver to be connected to any transmitter. Since we have bidirectional lightpaths, a transmitter/receiver pair together called as a transponder will be used for both add and drop.

Wavebands of transponders at a node are assigned in a random fashion as follows: For $T \leq B$, each transponder is assigned to a waveband randomly out of B wavebands without assigning the same waveband twice. For $T > B$, there are $\lfloor T/B \rfloor$ transponders assigned to each waveband, and the remaining $T \mod B$ transponders are assigned wavebands randomly in the same fashion. Upon a lightpath request arrival, the route is calculated by running a modified Dijkstra's shortest path algorithm on a certain graph (see Section III) and if a possible route is found the lightpath is established and the graph is updated; otherwise the call is blocked.

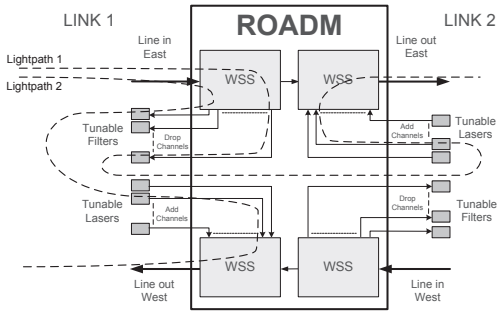

Fig. 2. SPL Model.

III. Graph Model & RWA Algorithms

A. The Augmented Graph

We create an augmented graph consisting of W layers, one corresponding to each wavelength. A similar multi-layer graph is used in [11] but we need a more complex graph for the reasons explained in the following paragraphs. The number of nodes in the graph is $4LW$. The graph consists of directional links but the path calculated is established for a bi-directional lightpath. We call the directional links in the augmented graph as **connections** to distinguish them from the links in the actual

network. We create the graph in three steps. In the first step we create each wavelength layer of the graph. In the second step, we connect the auxiliary source and destination nodes to the graph. In the third step, we connect the different layers by creating the connections corresponding to possible wavelength conversions at an intermediate node by adding and dropping. After running the shortest path algorithm on the graph, we get the route as well as the wavelength. Transponder selection at the source and destination nodes or at any intermediate node where an add/drop occurs is done in a random fashion. We denote the cost of a directional connection from node i to node j in the augmented graph by $C(i,j)$. We now explain these steps in detail.

Step 1: We have two subnodes for a node n for each of its degrees. One of the subnodes is the ingress subnode to which a directional link enters, and the second one is the egress node from which an outgoing link starts. We denote ingress and egress subnodes of degree t of node n at graph layer w by $S^w_{n,t,i}$ and $S^w_{n,t,e}$, respectively, where $1 \leq t \leq D_n$. We show the original network that we use as an example in Fig. 3 (a) and the subnodes corresponding to all 4 nodes in the original network are shown in Fig. 3 (b). n_1 and n_4 have 4 subnodes whereas n_2 and n_3 have 6 subnodes (2 subnodes per degree). Since we adopt the SPL model for transponders, having subnodes corresponding to each degree of a node is mandatory. Additionally, since there can only be one add/drop at a node, we implement an O-E-O conversion by a directional connection from an ingress subnode at one layer to an egress subnode at another layer of the graph. Egress subnodes are only connected to the other nodes in the network (i.e., not to any other subnode of its own node). Hence, if a path crosses an egress subnode, it is guaranteed that it leaves that node without resulting in multiple O-E-O conversions within the same node. For a node n, every ingress subnode of one of its degrees is connected to every other egress subnode of the other degrees. Therefore, $C(S^w_{n,t_1,i}, S^w_{n,t_2,e}) = 0 \ \forall \ n, w; 1 \leq t_1, t_2 \leq D_n (t_1 \neq t_2)$. These connections correspond to bypass connections (i.e., no add/drop) at that intermediate node. Fig. 3 (c) shows the bypass connections for a 2-degree node and we can see the bypass connections in Fig. 3 (b) for the 3-degree nodes n_2 and n_3. A link l connecting nodes n and m in the physical network corresponds to a connection between the egress subnode of n to the ingress subnode of the node m and also between the egress subnode of m to the ingress subnode of the node n. For example, in Fig. 3 (b) we show the connections in opposite directions between the nodes n_1 and n_2. Such a connection within a layer exists only if that wavelength is available on that link. We do the cost assignment between the corresponding subnodes in the same layer w by the following formula.

$$C(S^w_{n,t_n,e}, S^w_{m,t_m,i}) = C(S^w_{m,t_m,e}, S^w_{n,t_n,i}) =$$

$$\begin{cases} \frac{L-U(w)}{L}\sigma & \text{if } U(w) < L \\ \infty & \text{if } U(w) = L \end{cases} \quad \forall \ n, m (n \neq m), w. \tag{1}$$

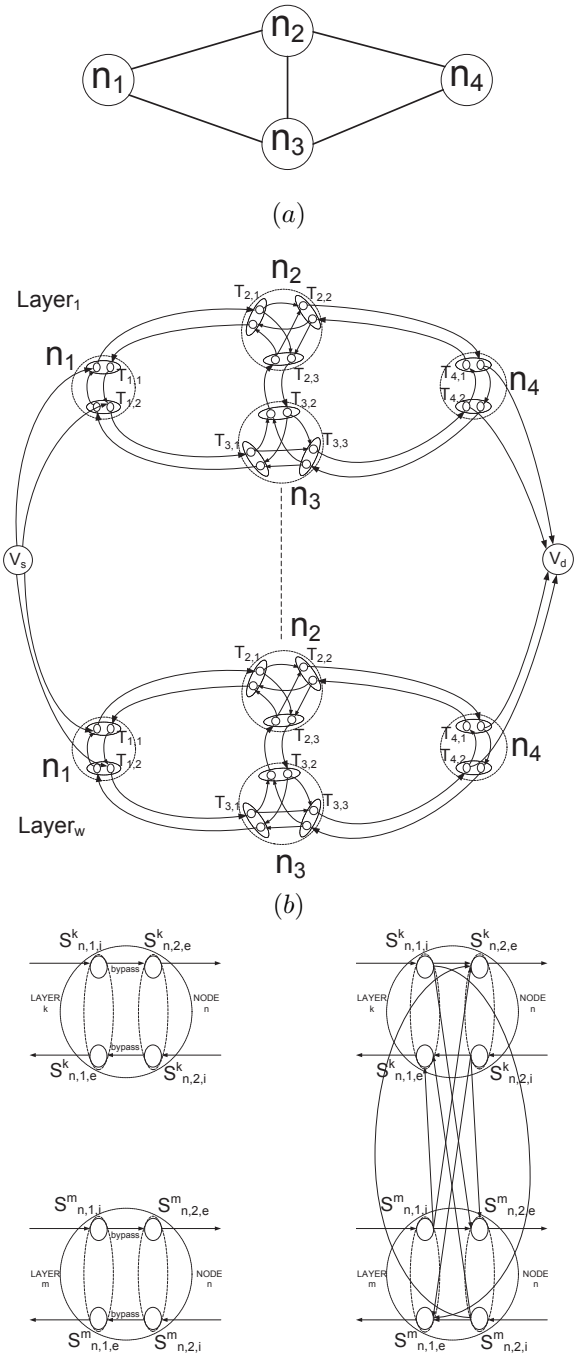

Fig. 3. (a) Original network (b) Augmented multi-layer graph; a 2-degree node in the augmented graph after establishing (c) bypass connections in Step 1, and (d) add/drop connections in Step 3.

where t_n and t_m are corresponding degrees of the nodes n and m to the actual link l, respectively; and σ is a scaling factor. $U(w)$ is the count of the overall usage of the wavelength w in the network ($0 \leq U(w) \leq L$); this information is based on the network state. With this cost assignment the more utilized a wavelength in the network is, the lower will be its cost, hence more likely to be chosen on a route. This is chosen because the most used wavelength assignment has been shown to perform very well [12].

After the cost assignment for each link is done at every layer, the graph looks like in Fig. 3 (b).

Step 2: We add nodes V_s and V_d to specify which nodes are the source and destination of the arriving lightpath. V_s is connected to every egress subnode of the source node s, and every ingress subnode of destination node d is connected to V_d in every layer w. For example, V_s is connected to every egress node of n_1, and every ingress node of n_4 is connected to V_d in Fig. 3 (b) if a lightpath is requested between n_1 and n_4. The costs of these connections are

$$C(V_s, S^w_{s,t_s,e}) = \frac{1}{Z(s,t_s,w)} \tag{2}$$

and

$$C(S^w_{d,t_d,i}, V_d) = \frac{1}{Z(d,t_d,w)}, \tag{3}$$

where $1 \leq t_s \leq D_s$ and $1 \leq t_d \leq D_d$. $Z(n,t,w)$ is the number available transponders in the degree t_n of node n and that can tune to wavelength w.

Step 3: In the last step, connections are formed between different layers. As we have seen in the previous section, a conversion takes place in an intermediate node n and it can be either within the same degree or other degrees of the same node. There exists a connection from an ingress subnode of t_1 in layer w_1 to the egress subnode of t_2 in layer w_2 and from the ingress subnode of t_2 in layer w_2 to egress subnode of t_1 in layer w_1. These connections for a 2-degree node are illustrated in Fig. 3 (d). We assign costs as below.

$$C(S^{w_1}_{n,t_1,i}, S^{w_2}_{n,t_2,e}) = C(S^{w_2}_{n,t_2,i}, S^{w_1}_{n,t_1,e}) =$$

$$\begin{cases} \frac{1}{\min(Z(n,t_1,w_1), Z(n,t_2,w_2))} & \text{if } t_1 = t_2 \\ \frac{1}{Y(n,t_1,w_1,w_2)} & \text{if } t_1 \neq t_2 \end{cases} \tag{4}$$
$$\forall\ n, w_1, w_2 (n \neq s,d)(w_1 \neq w_2),$$

where $Y(n,t_1,w_1,w_2)$ is the number of available transponder pairs, the first of which can tune to w_1 and the second to w_2, or vice versa. Functions Z and Y are chosen so that multihopping is done at the nodes which have higher number of available transponders for the purpose of not exhausting transponders of a node.

B. RWA Algorithms

The alternate multihop routing (AR-Multihop) algorithm is explained in Algorithm 1. We note that there are two connections in opposite directions in the augmented graph in one layer corresponding to one physical link in the network. Since we establish bidirectional calls, we prevent Dijkstra's algorithm from using both of these connections along a route at the same time by modifying the algorithm. Therefore, during a run of Dijkstra's algorithm, every time a subnode is reached via one such directional connection and it is included in the set for which shortest paths are already calculated, we make the connection in the opposite direction to have an infinite cost within the same layer w (i.e., if a subnode $S^w_{m,t_m,i}$ of node m is included in the set through a connection from another subnode ($S^w_{n,t_n,e}$) of node n, we set $C(S^w_{m,t_m,e}, S^w_{n,t_n,i}) = \infty$).

input : Network graph and network state
output: Routing and wavelength assignment for the lightpath request between the source and destination nodes (s,d)

Generation of the augmented graph G
  Create every layer of graph;
  Connect nodes V_s and V_d to the subnodes of s and d in each layer;
  Connect layers to each other by connecting the same nodes in different layers;
Run the modified Dijkstra's Shortest Path Algorithm to find paths from node V_s to every other node;
if *a path is found between V_s and V_d* **then**
  Trace the path from V_s to V_d;
  Establish the calls on each multihop on the calculated wavelengths;
  For the source and destination of each hop, choose the transponders randomly
else
  Block the call

Algorithm 1: Alternate multihop routing algorithm (AR-Multihop)

In order to compare the performance of multihopping with fixed routing, we modify our algorithm as follows. All routes between every source and destination pairs are initially computed according to minimum-hop routing. We create the augmented multilayer graph, however in this case each layer contains only the subnodes of physical nodes that are on the computed fixed route. For every lightpath request, this graph is created containing $4Wh$ nodes where h is the hop-length of the route. Costs of all the connections are calculated as in the previous case. Hence, this algorithm chooses the intermediate nodes that are best for multihopping on a fixed route. We name this algorithm as FR-Multihop. We have another algorithm which exhaustively searches for multihops on a fixed route. For a lightpath request arrival, it initially looks for an end-to-end wavelength-continuous route; if not found, it looks for an intermediate node starting with the next node along the fixed route to make the conversion (to establish a two hop route). Unless successful, it next looks for a 3-hop route, and so on. We name this algorithm as FR-Multihop-E.

In order to distill the benefits of multihopping alone (from the combination of multihopping and alternate routing), we compare the performance of our algorithm with an alternate routing algorithm without multihopping. We again modify our algorithm for this purpose by just skipping the third step of the graph generation procedure which creates the connections in the graph for multihopping. We call this algorithm AR. We also call the fixed routing without multihopping as FR.

IV. Numerical Results

We ran simulations on the 10-node ring network and the well-known NSFNet using 100000 call arrivals (10000 ar-

rivals at higher loads due to time constraints). In all of our simulations, we use $W = 16$. Overall blocking probability is calculated by taking the average of route blocking probability over every route (i.e., every source and destination pair). ρ is the load per route and per wavelength. Unless mentioned otherwise we use $\sigma = 0.2$ for the algorithms AR and AR-Multihop. The curves of FR-Multihop and FR-Multihop-E are very similar, so we only present FR-Multihop-E results in our graphs.

We first plot blocking vs. load for ring and NSFNet in Fig. 4 (a) and (b), respectively. In Fig. 4 (a), we see that FR gives the worst blocking and FR-Multihop-E improves the blocking compared to FR. Therefore, multihopping offers an advantage even for fixed routes. The blocking values of AR are lower than FR-Multihop-E, which shows that using alternate routes even without multihopping is more advantageous than having multihopping on a fixed route. AR-Multihop results in the lowest blocking values (significantly lower than AR) and the difference between the other curves is much larger with lower loads. For load $\rho = 0.03$, the ratio of the blocking values of FR and and AR-Multihop is 53. Therefore, the addition of multihopping in alternate routing improves the blocking significantly compared to only alternate routing. As the load increases, all of the curves merge to the same value. The same behavior is true for the NSFNet in Fig. 4 (b), AR-Multihop results in better blocking than the other algorithms. The curve of AR-Multihop increases in a linear fashion while the difference is larger with lower loads. However, the performance difference between AR and AR-Multihop is not significant in NSFNet compared to the ring. AR-Multihop and AR curves get closer after $\rho = 0.04$. We conclude that alternate routing offers advantage over all fixed routing methods with or without multihopping, but alternate multihop routing improves the blocking even further (except for higher loads after $\rho = 0.050$ for the NSFNet).

We now look into the performance of AR-Multihop when WTTs are utilized in the network (i.e., $\Theta = 16$). In Fig. 5 (a), we observe that AR and AR-Multihop curves are very close and they are both better than both of the FR algorithms. The gap between AR and FR curves is larger for lower loads. This is the same for NSFNet as seen in Fig. 5 (b) where we observe a larger gap between FR and AR curves. We conclude that when WTTs are used in the network multihopping with alternate routing is not as advantageous as when LTTs are used.

We compare the performance of the two FR algorithms and AR-Multihop in Fig. 6 by plotting blocking vs. number of transponders (T) for ring and NSFNet. We observe that the blocking for AR-Multihop decreases until $T = 8$ for the ring in Fig. 6 (a) for AR-Multihop with $\sigma = 0.2$ at a fast rate. After that point, it decreases slightly until $T = 16$ except a slight increase at $T = 14$. With a higher σ value of 1.0, AR-Multihop performance gets better for larger T values than 8 with the expense of higher blocking than with $\sigma = 0.2$ for $T \leq 8$. FR and FR-Multihop-E performance is continuously decreasing with T while the gap between the two curves is increasing. The

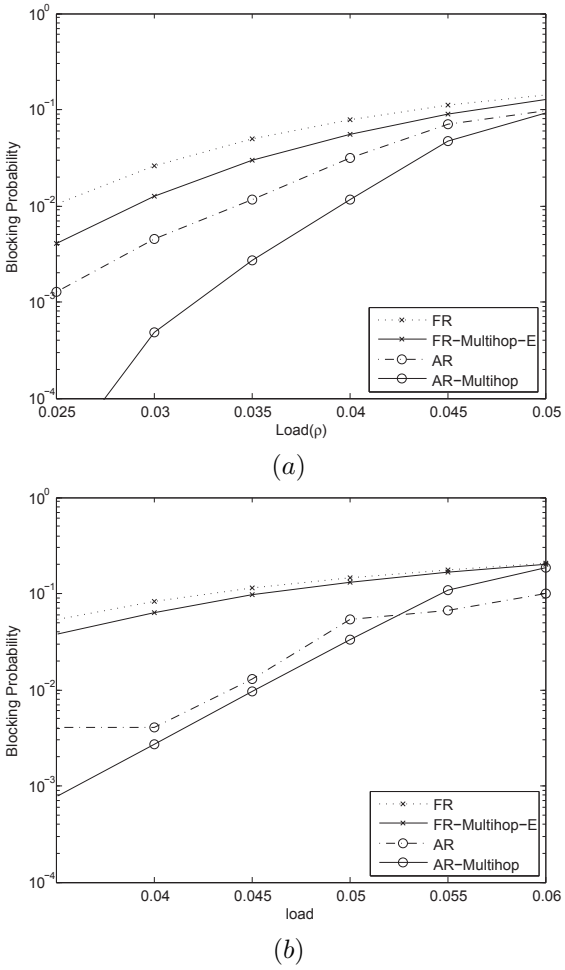

Fig. 4. Blocking probability vs. load (ρ) for $T = 8$ and $\Theta = 2$ in (a) ring (b) NSFNet.

difference between the curves of both FR algorithms and AR-Multihop becomes significantly high after $T = 6$. Therefore, the advantage of multihopping increases with higher T, and for lower T values multihopping exhausts the transponders in the network. In Fig. 6 (b), we see that AR-Multihop performs much better than both FR algorithms for NSFNet, especially for higher T values. After $T = 8$, blocking with AR-Multihop is at least 30 times lower than FR algorithms. FR and FR-Multihop-E curves are close until $T = 8$ but after that FR-Multihop-E starts performing better. We again conclude that multihopping offers the most advantage at higher T values when the transponder resources are more abundant.

V. Conclusion

We studied the performance of multihopping with O-E-O conversions along the route of a lightpath considering the use of limited tunable transponders in the reconfigurable nodes. We developed an alternate multihop routing algorithm to select a multihop route based on the availability and tunabilities of limited tunable transponders while considering the wavelength usage as well. We compared the performance of the AR-Multihop algorithm with fixed routing algorithms (with or

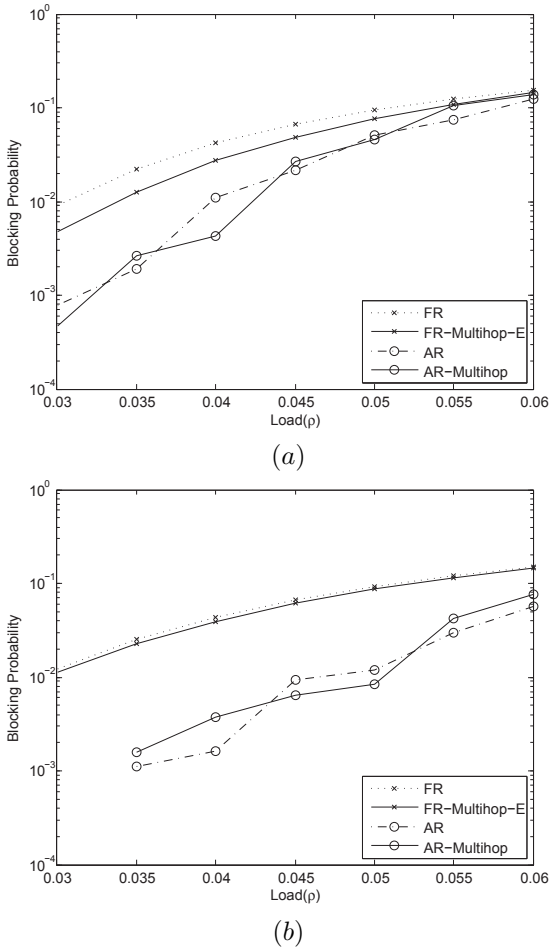

Fig. 5. Blocking probability vs. load (ρ) for $T = 8$ and $\Theta = 16$ in (a) ring (b) NSFNet.

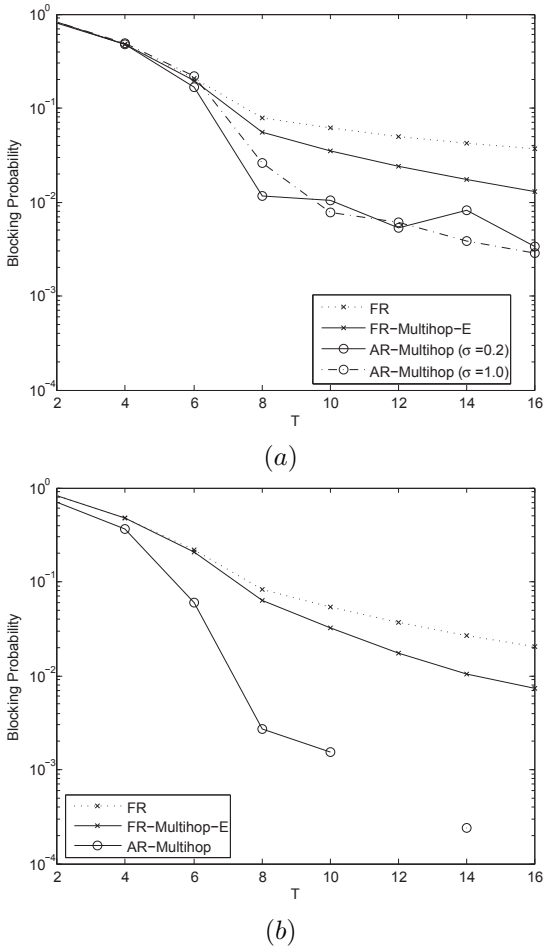

Fig. 6. Blocking probability vs. number of transponders (T) for $\Theta = 2$ and $\rho = 0.04$ in (a) ring (b) NSFNet.

without multihopping) and also with alternate routing without multihopping. We showed that the AR-Multihop algorithm is superior to all in terms of blocking when limited tunable transponders are used and the performance gap is quite large with lower loads (e.g., 53 times better for $\rho = 0.03$ in the ring network). The results confirm that alternate routing results in a better performance than fixed routing methods with or without multihopping, but when it is used with multihopping the performance is further improved in the case of limited tunable transponders. We also showed that multihopping results in better blocking with higher number of transponders when O-E-O conversions do not exhaust the transponders in the network.

ACKNOWLEDGMENT

This work was supported in part by NSF Grant CNS-0434956.

REFERENCES

[1] O. Turkcu and S. Subramaniam, "Blocking in reconfigurable optical networks," in *Proc. Infocom*, May 2007.
[2] Finisar. [Online]. Available: http://www.finisar.com
[3] G. Shen *et al.*, "The impact of number of transceivers and their tunabilities on WDM network performance," *IEEE Commun. Lett.*, vol. 4, no. 11, pp. 366–368, Nov. 2000.
[4] L. Parascbis, O. Gerstel, and R. Ramaswami, "Evaluation of tunable laser applications in metropolitan networks," in *Proc. OFC*, Feb. 2004.
[5] O. Turkcu and S. Subramaniam, "Blocking and waveband assignment in WDM networks with limited reconfigurability," in *Proc. OFC*, March 2007.
[6] S. Subramaniam, M. Azizoğlu, and A. K. Somani, "All-optical networks with sparse wavelength conversion," *IEEE/ACM Trans. Networking*, vol. 4, no. 4, pp. 544–557, Aug. 1996.
[7] X. Cao, V. Anand, and C. Qiao, "Waveband switching for dynamic traffic demands in multigranular optical networks," *IEEE/ACM Trans. Netw.*, vol. 15, no. 4, pp. 957–968, Aug. 2007.
[8] ——, "A study of waveband switching with multilayer multigranular optical cross-connects," *IEEE J. Sel. Areas Commun.*, vol. 21, no. 7, pp. 1081–1095, Sep. 2003.
[9] R. Izmailov, A. Kolarov, R. Fan, and S. Araki, "Hierarchical optical switching: A node-level analysis," in *Proc. HPSR'02*, May 2002, pp. 309–313.
[10] X. Chu and B. Li, "Dynamic routing and wavelength assignment in the presence of wavelength conversion for all-optical networks," *IEEE/ACM Trans. Networking*, vol. 13, no. 3, pp. 704–714, Jun. 2005.
[11] T. Ye *et al.*, "On-line integrated routing in dynamic multifiber IP/WDM networks," *IEEE J. Select. Areas Commun.*, vol. 22, no. 9, pp. 1681–1691, Nov. 2004.
[12] H. Zang, J. Jue, and B. Mukherjee, "A review of routing and wavelength assignment approaches for wavelength-routed optical WDM networks," *Optical Networks Magazine*, vol. 1, no. 1, Jan. 2000.